

Nickel-Catalyzed Enantioselective Reductive Conjugate Arylation and Heteroarylation via an Elementary Mechanism of 1,4-Addition

Luoqiang Zhang, Mengxin Zhao, Maoping Pu, Zhaoming Ma, Jingsong Zhou, Caiyou Chen, Yun-Dong Wu, Yonggui Robin Chi, and Jianrong Steve Zhou*



Cite This: *J. Am. Chem. Soc.* 2022, 144, 20249–20257



Read Online

ACCESS |



Metrics & More

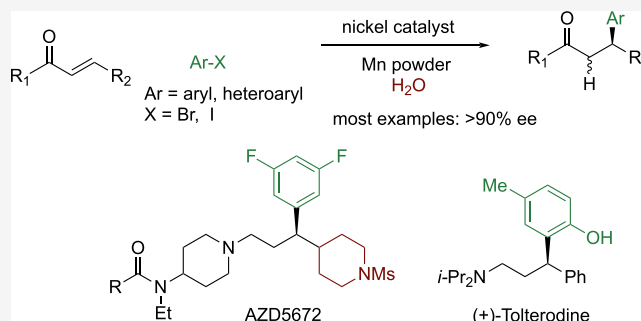


Article Recommendations



Supporting Information

ABSTRACT: A nickel complex of isoquinox promoted enantioselective conjugate arylation and heteroarylation of enones using aryl and heteroaryl halides directly. The reaction was successfully applied to stereoselective syntheses of *ar*-turmerone, chiral fragments of (+)-tolterodine and AZD5672. Mechanistically, experiments and calculations supported that an arynickel(I) complex inserted to enones via an elementary 1,4-addition.



INTRODUCTION

Metal-catalyzed asymmetric conjugate arylation of Michael acceptors constitutes an important family of C-C bond-forming reactions, which have been widely used in total synthesis of natural products and medicines. In the past, chiral copper catalysts have dominated in asymmetric conjugate addition of arylmetal reagents, for example, Li, Mg, Al, Zn, and so on (see Figure 1a).¹ For conjugate addition of aryl-nonmetal reagents, especially air-stable arylborons, however, stereoselective examples catalyzed by copper still remain limited.^{2,3} In comparison, 4d transition metals Rh⁴ and Pd⁵ have met great success in promoting conjugate addition of both organoboron reagents (Figure 1b). In particular, the

rhodium-catalyzed Hayashi–Miyaura reaction has become the state-of-the-art in asymmetric metal catalysis in terms of excellent levels of stereocontrol and substrate diversity, for example, including both cyclic and acyclic acceptors. It has been utilized in the preparation of multiple chiral pharmaceuticals on kilogram scales.⁶

Aryl halides are electrophilic reagents. Direct use of aryl halides certainly has practical benefits. This major family of carbon electrophiles are readily available and benchtop-stable. In comparison, some organometallic reagents (e.g., Grignard reagents) are incompatible with relatively acidic groups and also are less tolerant of polar groups (e.g., aldehydes and ketones), especially when room temperature or heating is applied. This also avoids preparation of arylboron reagents. Regioselective preparation of some arylboron reagents uses arylmetal reagents (e.g., those of Mg and Li) or aryl halides as a starting material. Additionally, transmetalation of some arylborons requires strong bases under catalytic conditions.

In 2013, Weix and co-workers first disclosed nickel-catalyzed reductive addition of aryl halides to enones, in the presence of trialkylsilyl chlorides and manganese powder.⁷ The reaction proceeded via η^3 -1-siloxyallylnickel species and subsequent coupling with aryl halides, rather than elementary insertion of arynickel species. However, achieving an intermolecular

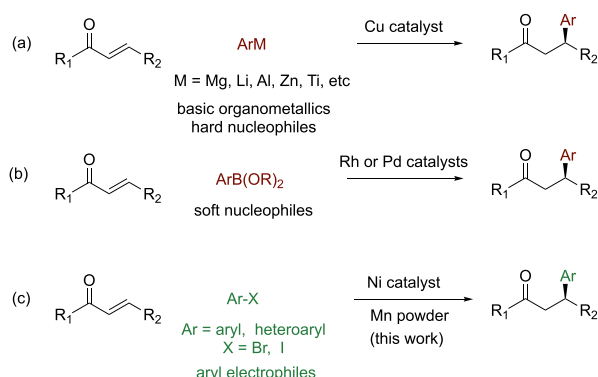


Figure 1. Examples of metal-catalyzed enantioselective conjugate addition: (a) Cu-catalyzed addition of reactive arylmetal reagents; (b) Rh- and Pd-catalyzed addition of arylboron reagents; (c) Ni-catalyzed reductive addition of aryl halides.

Received: May 29, 2022

Published: October 31, 2022

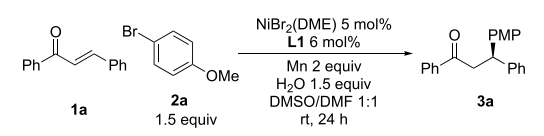


reductive arylation has proved to be challenging.⁸ Herein, we report such an enantioselective variant under very mild conditions (Figure 1c). It should be pointed out that organometallic reagents (M = Mn or Zn) are not directly involved in the C–C bond formation herein.⁹

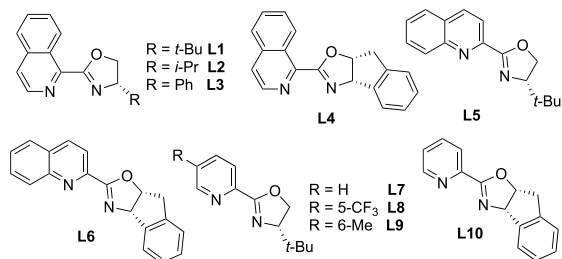
CONDITION OPTIMIZATION

Initially, we examined a model reaction between 4-bromoanisole **2a** and (*E*)-chalcone **1a** to identify suitable nickel catalysts and conditions. After many trials, we established an efficient protocol using a precatalyst of NiBr₂(DME) and isoquinox **L1**, manganese powder, and 1.5 equiv of H₂O in a 1:1 mixed solvent of dry DMSO and DMF. Thus, desired product **3a** was generated in 86% yield and 92% enantiomeric excess (ee) after 24 h at rt (Table 1, entry 1).

Table 1. Condition Optimization of Asymmetric Reductive Arylation of (*E*)-Chalcone (Calibrated GC Yields on 0.1 mmol Scale in 0.3 mL of Solvents)



Entry	Conditions	Conv. of 1a (%)	Yield of 3a (%)	Ee (%)
1	L1	96	86	92
2	L2	64	49	79
3	L3	52	39	80
4	L4	45	41	87
5	L5	43	23	90
6	L6	32	18	94
7	L7	19	10	86
8	L8	21	18	77
9	L9	10	6	89
10	L10	18	12	82
11	[Ni] 2.5 mol%	52	48	92
12	DMF solvent	44	36	93
13	DMSO solvent	75	41	91
14	without H ₂ O	94	7	64
15	H ₂ O 3 equiv	82	69	92
16	50 °C	81	19	87



With regard to isoquinox ligands,^{4k,10} changing the sidearm from the *tert*-butyl group to isopropyl, phenyl, and indanyl (**L2**–**L4**) led to moderate yields (41–49%) and slightly lower stereoselectivity (79–87% ees), as shown in entries 2–4. Among other dinitrogen chelators, quinox **L5**–**L6** and pyrox **L7**–**L10** resulted in very low yields of **3a** (6–23%), albeit in good-to-excellent ees (entries 5–10).

The additive of water proved essential. Without water, **3a** was produced in only 7% yield and 64% ee. Most chalcone **1a** was thus sidetracked to form trimeric side products (via sequential nickel(0)-catalyzed reductive coupling of enones, conjugate addition to a third chalcone, aldol cyclization to form cyclopentanols, and final dehydration)¹¹ (entry 11). Addition of 3 equiv of H₂O led to lower yield of the product

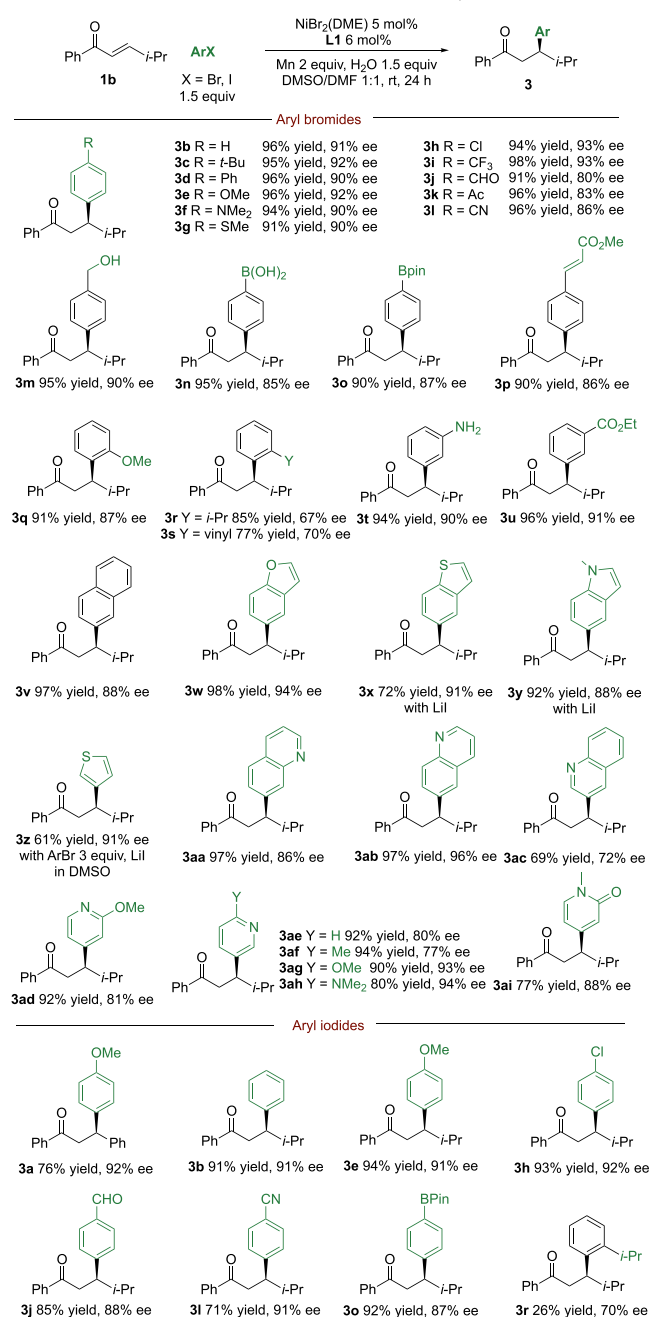
(entry 12). Additionally, a mixed solvent of 1:1 DMSO/DMF was optimal; only ~40% yield was obtained in pure DMF or DMSO in comparison (entries 13 and 14). In DMF, only 44% enone was consumed after 24 h; a significant amount of side product, arene was detected after 24 h. The enone conversion was 75% in DMSO, along with a significant amount of the trimeric side products. In 1:1 DMF/DMSO, the excess of aryl bromide remained after 24 h, along with small amounts (<5%) of anisole and biaryl (for details, see the Supporting Information).

SUBSTRATE SCOPE

With the optimized conditions in hand, we first examined the scope of (hetero)aryl bromides with (*E*)-enone **1b** (Scheme 1). A wide range of aryl bromides bearing both electron-donating (**3b**–**g**, **3m**) and electron-withdrawing substituents (**3h**–**i**, **3p**) reacted smoothly to afford desired products in 80–93% ees. Notably, aryl bromides carrying aldehyde, ketone, and nitrile groups gave slightly lower ees. Importantly, the condition was also compatible with benzyl alcohol (**3m**), aniline (**3t**), aryl boronic acid, and aryl Bpin (**3n**–**o**), but not phenol. The reaction also worked well with 2-bromoanisole (**3q**), but hindered aryl bromides possessing *o*-*i*Pr and *o*-vinyl groups provided only 67% ee and 70% ee (**3r**–**s**). To our delight, many heteroaryl bromides proved to be suitable electrophiles, including derivatives of benzofuran (**3w**), benzothiophene (**3x**), indole (**3y**), thiophene (**3z**), quinoline (**3aa**–**ac**), pyridine (**3ad**–**ah**), and pyridone (**3ai**); parent 3-pyridyl bromide also provided adduct **3ae** in 80% ee. Some bromides of electron-rich heteroarenes, thiophene, benzothiophene, and indole, reacted rather sluggishly; 1 equiv of LiI was added to ameliorate this problem. In terms of reactivity and selectivity, electron-neutral and electron-rich aryl halides (Br and I) provided similar isolated yields and ees, but some electron-deficient aryl iodides gave slightly better ees than bromides (**3j**, **3l**). Hindered *o*-iodocumene, however, afforded product **3r** in poor yield, along with significant biaryl formation.

Next, we examined the scope of α,β -enones, using 4-tolyl bromide (4-tolyl iodide was used in some sluggish reactions) (Scheme 2a). Conjugate arylation to parent (*E*)-chalcone furnished β,β' -diaryl ketone **4a** in 87% yield and 92% ee. On β -aryl rings of chalcones, both electron-donating and -withdrawing substituents can be present such as phenoxy (**4c**), ester (**4d**), methoxy (**4e**), phenyl (**4f**), diphenylamino (**4g**), methylthio (**4h**), fluorine (**4j**), and trifluoromethyl groups (**4k**). Notably, the presence of an *ortho*-anisyl group at the β -position slightly decreased the stereoselectivity (86% ee for **4i**), while an *o*-tolyl group reduced the value to 57% ee. Moreover, β -aryl rings of chalcones can be substituted with heteroaryl rings, for example, thiophene, furan, pyridine, and quinoline (**4m**–**q**). For some substrates above, especially chalcones having β -electron-deficient aryl groups and heteroaryl rings, switching from aryl bromides to iodides significantly improved chemical yields and minimized the trimeric side products formation. Notably, a 2,4-dienone led to exclusive β -arylation in 91% ee (**4r**). Moreover, β -positions of (*E*)-enones can have isopropyl, methyl (**4s**), *n*-hexyl (**4t**), other alkyl chains carrying ester and phthalimide groups (**4u**–**v**), and an *N*-benzylpiperidyl group (**4w**). Finally, arylation of (*E*)-2-benzylidenetetralone and its 4-oxa derivative generated products **4t** and **4y** as 1:1 mixtures of diastereomers, with both isomers formed in 91 and 90% ee, respectively. We also attempted arylation of α -

Scheme 1. Substrate Scope of (Hetero)aryl Bromides and Iodides in Asymmetric Conjugate Arylation (Isolated Yields on 0.1 mmol Scale in 0.3 mL of Solvents)



methylchalcone using 4-tolyl bromide, which resulted in low conversion and low yield, along with a significant amount of biaryl.

As shown in Scheme 2b, enones can have different α' -aryl groups containing *ortho*-groups (**5a**) and electron-donating and -withdrawing groups (**5b–f**). On the α' -position, aryl rings can be replaced by heteroaryls including furan, thiophene, benzothiophene, thiazole, and 2-methoxypyridine (**5i–n**). Again, some reactions using heteroaryl iodides proceeded more efficiently than the corresponding bromides (**5l** and **5m**). (*S*)-(+)-*ar*-turmerone **5o** is a key component of turmeric essential oil. Recent studies found that it possessed promising neuroprotective properties.¹² Without modification of the conditions, regioselective tolylation of dialkenyl ketone **1o**

proceeded exclusively at the less-substituted alkene to give (*S*)-*ar*-turmerone **5o** in 93% ee (Scheme 2c).

In the reaction of isopropyl styryl ketone with 4-tolyl bromide, only 36% conversion was observed after 24 h, giving product **5p** in 27% yield and 54% ee. To our gratification, switching from isoquinox **L1** to quinox **L6** and employing 4-tolyl iodide significantly improved the result, giving **5p** in 72% yield and 93% ee (Scheme 2d). Similarly, the new procedure also enabled stereoselective arylation of enones bearing other α' -alkyl groups such as *t*Bu and *i*Bu (**5q** and **5r**).

SYNTHETIC APPLICATION

To demonstrate synthetic utility, we have applied the new reaction in formal syntheses of (+)-tolterodine,¹³ a blockbuster drug for the treatment of urinary incontinence (Figure 2). Thus, 4'-methoxychalcone was arylated with 2-iodo-4-methylanisole, and subsequent Baeyer–Villiger oxidation yielded ester **6a**, a synthetic precursor to (+)-tolterodine, in 70% yield with 87% ee in two-steps. Similarly, the two-step sequence was applied to conjugate arylation using 3,5-difluorophenyl bromide to provide **6b** in 86% yield and 96% ee. The latter is a key intermediate en route to AZD5672,¹⁴ a drug candidate for the treatment of rheumatoid arthritis.

MECHANISTIC STUDIES

We have carried out some experiments to probe the reaction mechanism (Figure 3): (a) conjugate 4-tolylation of enone **1m** in the presence of D₂O resulted in products **4m–d** with deuterium at both α positions in nearly 1:1 ratio. A nondeuterated sample of **4m**, when added to a live catalytic arylation of enone **1a**, 4-anisyl bromide, and 1.5 equiv D₂O, no deuteration was detected in recovered **4m**. Thus, after 1,4-addition, an *O*-bound nickel enolate undergoes a non-stereoselective protonation (Figure 3a); the resulting hydroxonickel(I) complex is directly reduced to Mn powder or it is converted to a bromide complex, which was then reduced. (b) In catalytic tolylation of chalcone **1a** (*Z/E* 10:1) (Figure 3b), the (*E*)-isomer was depleted after 2 h, after which the *Z/E* ratio was maintained at 99.8:0.2 in both reactions. The kinetics showed that 4-tolyl iodide reacted much faster than the bromide; for instance, the reaction of ArI reached >90% conversion of the enone after 10 h, while only 40% conversion was seen in that of ArBr. Importantly, in both reactions of 4-tolyl bromide and iodide, product **4a** was formed in identical 92% ee. We reasoned that in situ formed MnX₂ catalyzed slow *Z/E* isomerization of (*Z*)-**1a** to form (*E*)-**1a** in low concentrations, the latter being the reactive substrate for catalytic arylation. (c) Catalytic arylation of cyclic enones, for example, 2-cyclopentenone and 2-cyclohexanone, led to ~50% conversion of enones, and *racemic* products **4z** and **4z'** were produced in poor yields, along with a significant amount of biaryl (Figure 3c).

To gain insights of the reaction mechanism, we prepared arylnickel^{II} complex (bipy)Ni(Ar)Br **7** (Ar = *o*-iPrC₆H₄)¹⁵ and subjected it to stoichiometric reactions with 3 equiv of enone **1b** (Figure 4a). With Mn powder, *rac*-**3r** was produced in 60% yield after 8 h, along with 5% cumene and 2% biaryl. In comparison, almost no *rac*-**3r** (3%) was detected without Mn, indicating that Mn reduction was essential for aryl transfer. Several additional observations were made: (1) prestirring of the nickel complex of bipy **7** with 2 equiv of isoquinox **L1** at rt. for 2 h caused little change to the outcome of the arylation

Scheme 2. Asymmetric Conjugate (Hetero)arylation of Enones with Structural Variations: (a) (Hetero)aryl, Alkenyl, and Alkyl Groups at the β -Position; (b) (Hetero)aryl, (c) Alkenyl, and (d) Alkyl Groups at the α' -Position (Isolated Yields on 0.1 mmol Scale in 0.3 mL of Solvents)

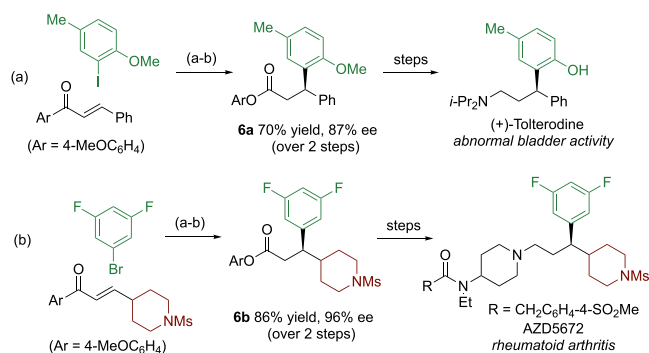
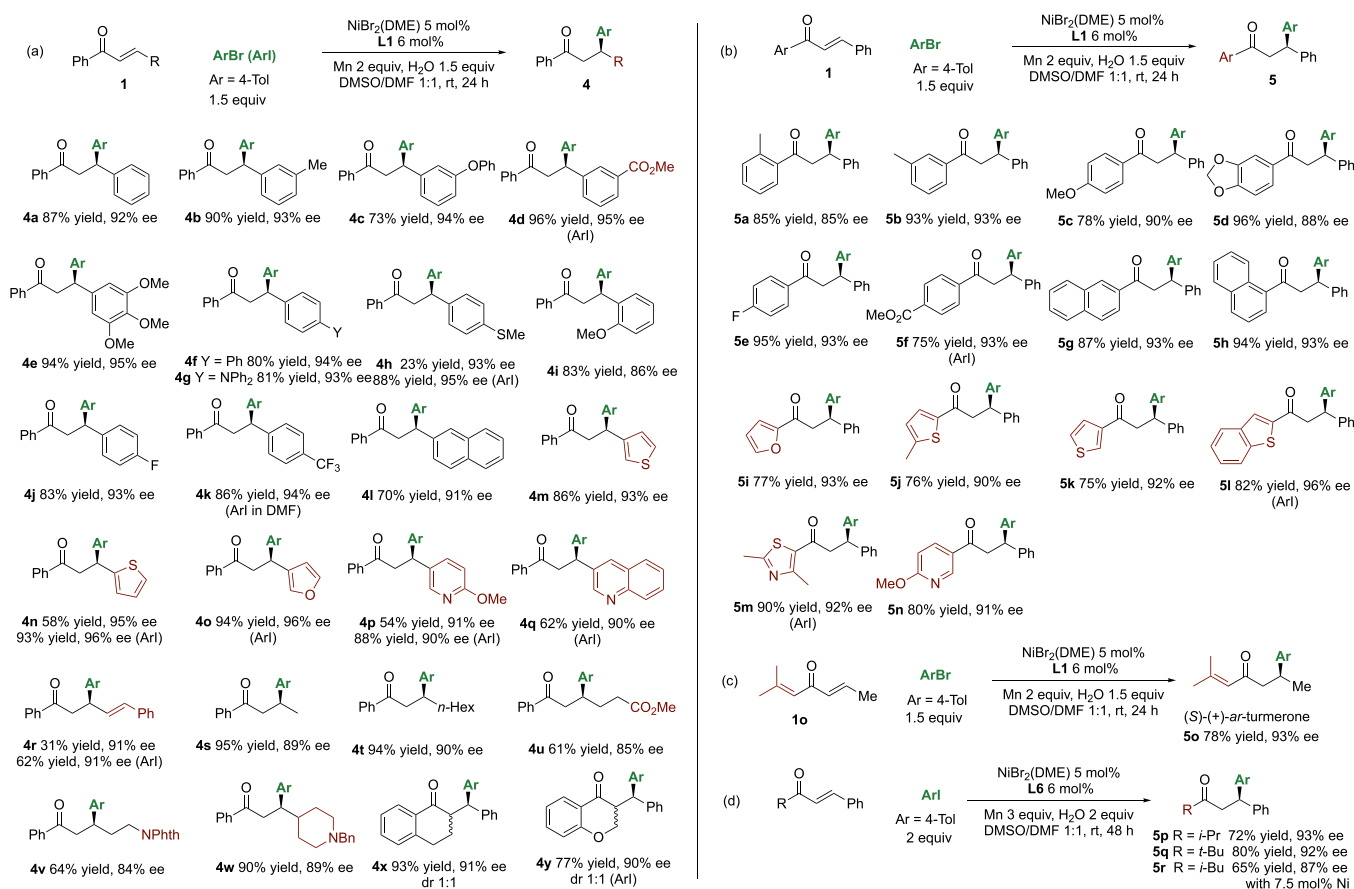
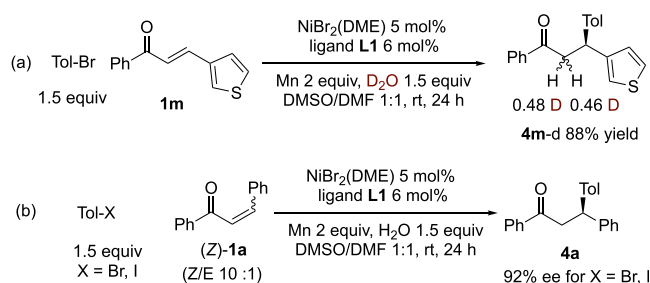


Figure 2. Formal syntheses of (a) (+)-tolterodine and (b) AZD5672 (isolated yields on 0.1 mmol scale in 0.3 mL of solvents for catalytic arylation): (a) enone (1 equiv), ArX (1.5 equiv), 5 mol % $\text{NiBr}_2(\text{DME})$, 6 mol % **L1, Mn powder (2 equiv), H_2O (1.5 equiv), 1:1 DMSO/DMF, rt, 24 h; (b) TsOH- H_2O (0.2 equiv), mCPBA (3 equiv), DCM, 35 °C, 36 h.**

(66% yield; 4% ee), indicating that ligand exchange on the nickel complex was slow at rt. (2) When 30 mol % MnBr_2 and 36 mol % ligand **L1** were added to the stoichiometric arylation of complex **7**, it gave *racemic* **3r** in 55% yield, suggesting that complex (**L1**) MnBr_2 did not participate in the stereoselective aryl transfer to enones.

We also prepared isoquinox complex (**L1**) $\text{Ni}^{\text{II}}(o\text{-iPrC}_6\text{H}_4)\text{Br}$ **8** as a 1:1 *cis/trans* isomer. The large *o*-iPr group is essential to preventing decomposition via biaryl formation. A stoichio-



Time (h)	X = Br		X = I	
	Conv (%)	4a (%)	Conv (%)	4a (%)
2	7	2	20	13
4	23	12	52	31
10	40	30	93	83
24	52	38	97	86

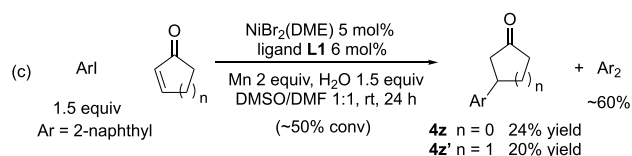


Figure 3. Mechanistic studies using different enones in catalytic arylations (0.1 mmol scale in 0.3 mL of solvents): (a) arylation of enone **1 m using D_2O ; (b) catalytic arylation of chalcone (*cis/trans* 10:1) using 4-tolyl halides; (c) catalytic arylation using 2-cyclopentenone and 2-cyclohexenone.**

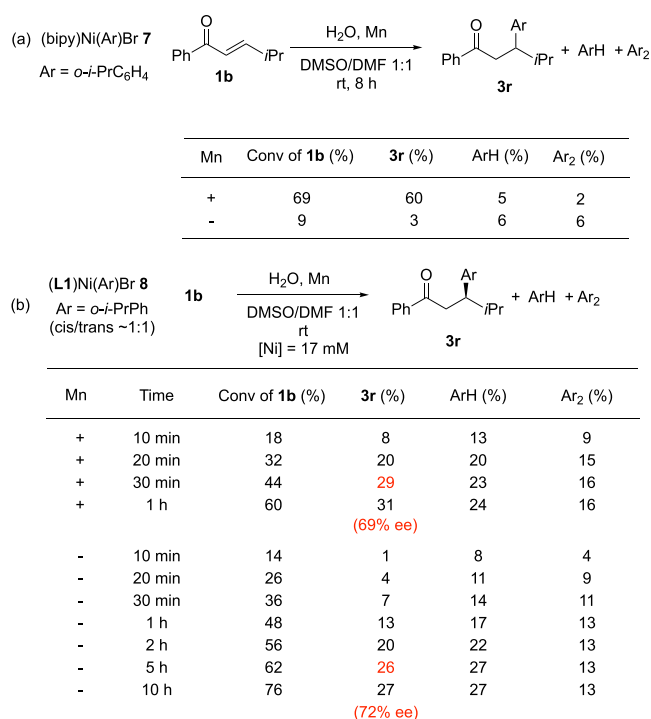


Figure 4. Stoichiometric reactions using nickel complexes. (a) Arylation of enone **1b** (0.15 mmol) with complex **7** (0.05 mmol), water (0.08 mmol), and Mn (0.25 mmol) in 1:1 DMSO/DMF (0.3 mL) (full conversion of **1b** is 300%). (b) Arylation of enone **1b** (0.5 mmol) under conditions similar to catalytic reactions (5 mol % nickel): complex **8** (0.025 mmol), water (0.75 mmol), and Mn (1.0 mmol) in 1:1 DMSO/DMF (1.5 mL).

metric reaction of complex **8**, enone **1b**, and Mn powder (see Figure 4b), under conditions similar to catalytic arylations ([Ni] = 17 mM), gave **3r** in ~30% yield (69% ee) after 30 min. However, the arylation without Mn was much slower, providing **3r** in ~30% yield (72% ee) after 5 h. As a side note, the stoichiometric arylation at a high nickel concentration (170 mM) gave the product in 40% ee, suggesting that a bimetallic complex of nickel (possibly with a bridging bromide ligand) may exist at high nickel concentrations and lead to a less stereoselective pathway. When the catalytic reaction of *o*-*i*-PrC₆H₄Br and enone **1b** was conducted with 50 mol % nickel ([Ni] = 170 mM), the selectivity of **3r** also dropped to ~40% ee (see the Supporting Information).

Mn reduction of complex **8** (with a maximal absorbance at 520 nm) was monitored by UV-ultra red spectroscopy (see Figure 5). Clearly, a putative complex (L1)Ni^I(*o*-*i*-PrC₆H₄) **9** (540 nm) was produced quickly within 2–10 min, which eventually transformed to a solvated complex of (L1)Ni⁰ (550 nm). The latter was identified in comparison with (L1)-Ni⁰(cod). Organic byproducts were identified to be mainly cumene and a small amount of biaryl. Reduction with zinc dust was faster than Mn reduction and showed a similar kinetic profile.

Surprisingly, we found that complex **8** itself slowly decomposed in 1:1 DMSO/DMF with a half-life of ~1 h to give complex **9** and biaryl (as the main organic byproduct). The reaction probably proceeds via a sequence of aryl exchange, diaryl reductive elimination, and bromine abstraction by (L)Ni⁰ from complex **8** to form complex **9**, as depicted in eqs 1 and 2 (see the Supporting Information). This explains

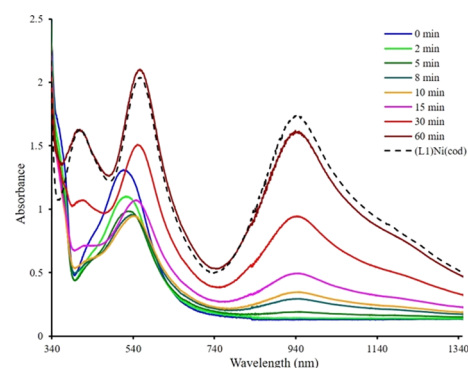
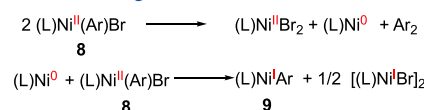


Figure 5. Kinetics of Mn reduction of (L1)Ni(*o*-*i*-PrC₆H₄)Br **8** as monitored by UV-ultra red spectroscopy.

slow formation of product **3r** from complex **8** even in the absence of Mn (see Figure 4b).



Next, we conducted electron paramagnetic resonance (EPR) analysis to detect elusive complex **9** via in situ zinc reduction of complex **8** in 1:1 DMSO/DMF (Figure 6a). MnBr₂ produced

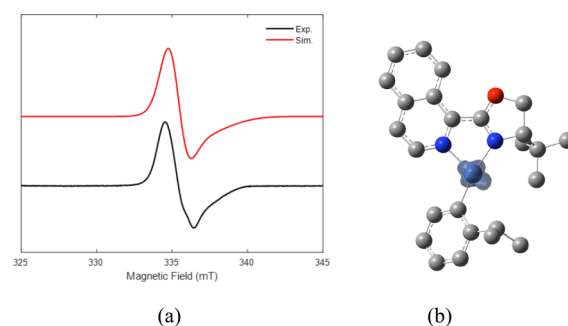


Figure 6. Characterization of (L1)Ni^I(*o*-*i*-PrC₆H₄) **9**. (a) X-band EPR spectrum of complex **9** collected in frozen 1:1 DMSO/DMF at 173 K (microwave frequency 9.422 GHz, power 0.6325 mW, modulation amplitude 2 G, and modulation frequency 1 mT/100 kHz) and a simulated spectrum (parameters used for simulation: *g* = 1.981, 1.996, 1.996). Hyperfine couplings from nitrogen atoms were unresolved. (b) DFT-computed (M06L/6-31G*) spin density plot of complex **9**.

in the Mn reduction interfered with the EPR signal. The EPR spectrum of complex **9** acquired at 173 K displayed anisotropy (*g* = 1.981, 1.996, 1.996) expected for a nickel-centered radical, rather than an organic radical delocalized in the isoquinox ligand. Density functional theory (DFT) calculations confirmed that the majority of the spin density resided on nickel (Figure 6b).¹⁶

DFT CALCULATIONS

We have conducted DFT calculations on elementary addition of putative species (L1)Ni^I(Ph) **9** to enone **1b** to understand the origin of its enantioselectivity. Geometry optimization calculations were performed at the M06L, SMD(DMF)/Def2-TZVP level of theory, using the SDD effective core potential basis set for Ni and 6-31G(d,p) basis set for other atoms. The alkene-bound complex is 6.6 kcal mol⁻¹ lower in Gibbs free energy than any ketone-bound structure. Assuming that these ground-state structures are quickly interconverting, we chose

the alkene complex as a reference point to compare relative energies of transition states in Figure 7. Among four transition

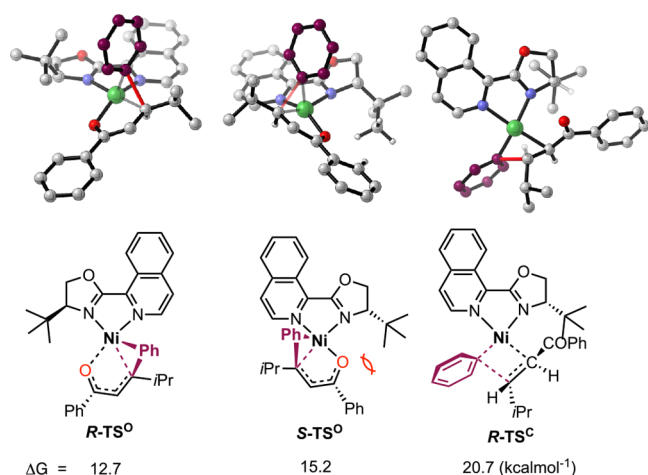


Figure 7. Calculated transition states and relative free energies for elementary 1,4-addition and 1,2-addition of (L1)Ni^I(Ph) **9** to enone **1b**. The migrating phenyl ring is highlighted in crimson in the ball-and-stick representation and the nascent C-C bond is marked in crimson; nickel, oxygen, and nitrogen atoms are marked in green, red, and blue, respectively.

states for 1,4-addition that we have identified, two lowest-energy ones **R-TS**⁰ and **S-TS**⁰ are shown, along with a transition state for 1,2-addition of the ketone **R-TS**^C.

Structures **R-TS**⁰ and **S-TS**⁰ are six-membered cyclic transition states for 1,4-addition,³ each possessing a migrating phenyl group above the coordination plane; they have Gibbs free energies of 12.7 and 15.2 kcal mol^{−1}, respectively (note: the barrier from a ketone-bound structure to **R-TS**⁰ is 6.1 kcal mol^{−1}). We conclude that **S-TS**⁰ is destabilized to alleviate close contact between the α'-Ph group of enone **1b** and *t*-butyl group of **L1** (both pointing downward). The energy gap of two TSs is 2.5 kcal mol^{−1}, which is expected for a reaction giving 91% ee. In comparison, structure **R-TS**^C for classical 1,2-addition across the olefin has a much higher energy of 20.7 kcal mol^{−1}. As a side note, simple 1,2-addition of the ketone has an inhibitory barrier of ~30 kcal mol^{−1}.

The cyclic transition states of 1,4-addition are instrumental to understanding some key experimental observations: (a) Enone (*Z*)-**1a** having a *cis*-β-substituent encountered difficulties in aryl addition owing to steric interactions. (b) The reacting enones must have *s*-cisoid conformers during aryl transfer, so cyclic 2-enones, being locked in *s*-transoid conformers, failed to produce enantioenriched adducts under the catalytic conditions (e.g., formation of racemic **4z** and **4z'** in low yields via another pathway in Figure 3c). (c) Large *ortho* groups on migrating aryl groups have a detrimental effect on the stereoselectivity; for example, aryl halides with *o*-iPr and *o*-vinyl groups provided products **3r-s** in moderate 70% ee. (d) For tolylation of an enone containing an α'-iPr group leading to product **5p**, the energy gap of two cyclic TSs on Ni/isoquinox **L1** was calculated to be 1.2 kcal mol^{−1}, consistent with observed 54% ee; switching to quinox **L6** boosted the selectivity to 93% ee. DFT calculations revealed that the large indanyl ring of **L6** raised the energy of the disfavored **S-TS**⁰ in order to avoid close contact with the *i*Pr group, which consequently increased the energy gap of two diastereomeric TSs to 2.8 kcal mol^{−1} (see the Supporting Information for

details of DFT calculations). (e) We have calculated three 1,4-addition pathways of enone **1b** using complexes (L1)Ni^I(Ar), (L1)Ni^{II}(Ar)⁺, and (L1)Ni^{II}(Ar)Br (Ar = *o*-iPrPh) leading to the major (*R*)-isomer. The barriers were 10.4, 21.3, and 32.9 kcal mol^{−1} respectively, which is consistent with fast arylation by neutral arylnickel^I (for details, see the Supporting Information of DFT calculations). The high barrier for cationic d⁸ arylnickel^{II} complexes of bipy-type ligands originates from a tendency to assume square-planar geometry (i.e., ground-state stabilization).^{16a}

DISCUSSION

Putting all the information together, we constructed a catalytic cycle for the reductive arylation of enones (Figure 8). After

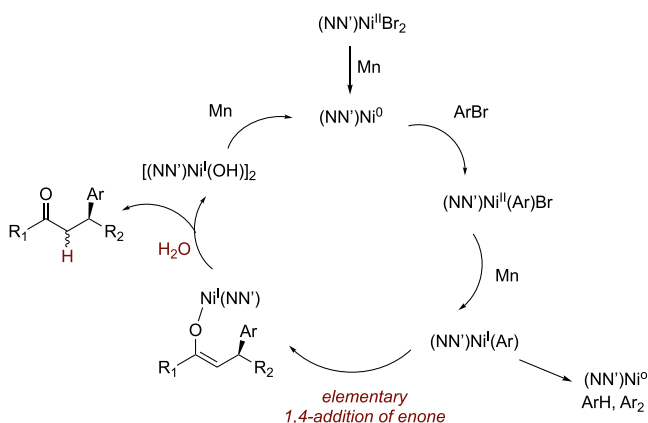


Figure 8. Proposed catalytic cycle.

oxidative addition of ArBr, (L1)Ni^{II}(Ar)Br was reduced by Mn powder to (L1)Ni^I(Ar). The latter underwent fast 1,4-addition to enones, and the resulting nickel O-enolate was hydrolyzed by water to release the final product. Finally, Mn reduction of either (L1)Ni^I(OH) (or its dimer) or (L1)Ni^I(Br) (or its dimer) completed the catalytic process.

Why do 3d late transition metals nickel and copper^{17,3,16} participate in rare elementary 1,4-addition of α,β-unsaturated carbonyls? Nickel and copper have relatively smaller covalent radii (1.24 and 1.32 pm),¹⁸ and they are more oxophilic (electronegativity 1.9) than 4d congeners rhodium and palladium. In addition, the 3d orbitals in the first transition series are contracted because of their poor ability to shielding nuclear charges. Thus, 3d orbitals of mid-to-late groups do not mix very effectively with bound ligands. Consequently, the aryl complexes of nickel and copper can participate in facile 1,4-addition via six-membered cyclic TSs (typically <10 kcal mol^{−1}), provided that Michael acceptors can assume the *s*-cisoid conformation. Direct M-O bonding stabilizes the nascent enolate structures which is a key feature of the cyclic TS. In comparison, putative 1,2-addition at α,β-positions of enones on nickel and copper has high barriers (>20 kcal mol^{−1}). In contrast, 4d metals palladium and rhodium have larger covalent radii (1.39 and 1.42 pm), and they are more carbophilic (electronegativity 2.2). They have more diffused and extended 4d orbitals with relatively low energies to effectively interact with frontier molecular orbitals of alkenes (including those of enones). Therefore, aryl complexes of Pd and Rh exhibit a high propensity toward classical 1,2-addition of olefinic moieties of enones.¹⁹ The 1,4-addition also differs from classical Cu^I/Cu^{III} shuttling which operates in conjugate

addition of high nucleophilic diorganocuprates and copper-catalyzed conjugate addition of organometallic reagents of Li, Mg, Zn, Al, and so on.²⁰ A bimetallic complex (L)₂CuR•MgBr₂ was proposed to undergo reversible oxidative addition at the β carbon of a Michael acceptor with the newly formed enolate intimately stabilized by the bridging MgBr₂ preceding rate-limiting C-C reductive elimination.

CONCLUSIONS

In summary, we report a nickel-catalyzed enantioselective reductive (hetero)arylation of α,β -unsaturated ketones. The new reaction has several attributes: very mild conditions, excellent tolerance of polar groups and heterocycles, broad scope of (hetero)aryl halides, broad scope of enones, and excellent stereoselectivity across the board (>90% ee). Mechanistically, both experiments and DFT calculations supported that arlynickel(I) species inserted to enones via a cyclic transition state of 1,4-addition.

ASSOCIATED CONTENT

Supporting Information

The Supporting Information is available free of charge at <https://pubs.acs.org/doi/10.1021/jacs.2c05678>.

Experimental procedures and compound characterization (PDF)

NMR spectra (PDF)

DFT calculations (PDF)

AUTHOR INFORMATION

Corresponding Author

Jianrong Steve Zhou – State Key Laboratory of Chemical Oncogenomics, Guangdong Provincial Key Laboratory of Chemical Genomics, School of Chemical Biology and Biotechnology, Peking University Shenzhen Graduate School, Shenzhen 518055, China; orcid.org/0000-0002-1806-7436; Email: jrzhou@pku.edu.cn

Authors

Luoqiang Zhang – State Key Laboratory of Chemical Oncogenomics, Guangdong Provincial Key Laboratory of Chemical Genomics, School of Chemical Biology and Biotechnology, Peking University Shenzhen Graduate School, Shenzhen 518055, China; School of Chemistry, Chemical Engineering and Biotechnology, Nanyang Technological University, 637371, Singapore

Mengxin Zhao – State Key Laboratory of Chemical Oncogenomics, Guangdong Provincial Key Laboratory of Chemical Genomics, School of Chemical Biology and Biotechnology, Peking University Shenzhen Graduate School, Shenzhen 518055, China

Maoping Pu – Shenzhen Bay Laboratory, Gaoke Innovation Center, Shenzhen 518107, China; orcid.org/0000-0002-0745-9549

Zhaoming Ma – State Key Laboratory of Chemical Oncogenomics, Guangdong Provincial Key Laboratory of Chemical Genomics, School of Chemical Biology and Biotechnology, Peking University Shenzhen Graduate School, Shenzhen 518055, China

Jingsong Zhou – School of Chemistry, Chemical Engineering and Biotechnology, Nanyang Technological University, 637371, Singapore

Caiyou Chen – College of Chemistry and Molecular Sciences, Wuhan University, Wuhan 430072, China; orcid.org/0000-0001-7536-7139

Yun-Dong Wu – Shenzhen Bay Laboratory, Gaoke Innovation Center, Shenzhen 518107, China; Laboratory of Computational Chemistry and Drug Design, State Key Laboratory of Chemical Oncogenomics, Peking University Shenzhen Graduate School, Shenzhen Bay Laboratory, Shenzhen 518055, China; orcid.org/0000-0003-4477-7332

Yonggui Robin Chi – School of Chemistry, Chemical Engineering and Biotechnology, Nanyang Technological University, 637371, Singapore; orcid.org/0000-0003-0573-257X

Complete contact information is available at:

<https://pubs.acs.org/doi/10.1021/jacs.2c05678>

Notes

The authors declare no competing financial interest.

ACKNOWLEDGMENTS

We acknowledge financial support from Peking University Shenzhen Graduate School, State Key Laboratory of Chemical Oncogenomics, Guangdong Provincial Key Laboratory of Chemical Genomics, Shenzhen Bay Laboratory and Shanghai Key Laboratory for Molecular Engineering of Chiral Drugs for J.S.Z., the National Natural Science Foundation of China (NSFC 21933004) for Y.D.W., and Singapore National Research Foundation (NRF-CRP22-2019-0002) for Y.R.C. M.Z. (experiments) and M.P. (DFT calculations) are co-first authors. We thank Prof. Richard Webster for EPR experiments.

REFERENCES

- (1) (a) Luchaco-Cullis, C. A.; Hoveyda, A. H. Cu-Catalyzed Enantioselective Conjugate Addition of Alkylzincs to Cyclic Nitroalkenes: Catalytic Asymmetric Synthesis of Cyclic α -Substituted Ketones. *J. Am. Chem. Soc.* **2002**, *124*, 8192–8193. (b) Lee, K.-S.; Brown, M. K.; Hird, A. W.; Hoveyda, A. H. A Practical Method for Enantioselective Synthesis of All-Carbon Quaternary Stereogenic Centers through NHC-Cu-Catalyzed Conjugate Additions of Alkyl- and Arylzinc Reagents to α -Substituted Cyclic Enones. *J. Am. Chem. Soc.* **2006**, *128*, 7182–7184. (c) Brown, M. K.; May, T. L.; Baxter, C. A.; Hoveyda, A. H. All-Carbon Quaternary Stereogenic Centers by Enantioselective Cu-Catalyzed Conjugate Additions Promoted by a Chiral N-Heterocyclic Carbene. *Angew. Chem., Int. Ed.* **2007**, *46*, 1097–1100. (d) López, F.; Minnaard, A. J.; Feringa, B. L. Catalytic Enantioselective Conjugate Addition with Grignard Reagents. *Acc. Chem. Res.* **2007**, *40*, 179–188. (e) Alexakis, A.; Bäckvall, J. E.; Krause, N.; Pàmies, O.; Diéguez, M. Enantioselective Copper-Catalyzed Conjugate Addition and Allylic Substitution Reactions. *Chem. Rev.* **2008**, *108*, 2796–2823. (f) Harutyunyan, S. R.; den Hartog, T.; Geurts, K.; Minnaard, A. J.; Feringa, B. L. Catalytic Asymmetric Conjugate Addition and Allylic Alkylation with Grignard Reagents. *Chem. Rev.* **2008**, *108*, 2824–2852. (g) Hawner, C.; Li, K.; Cirriez, V.; Alexakis, A. Copper-Catalyzed Asymmetric Conjugate Addition of Aryl Aluminum Reagents to Trisubstituted Enones: Construction of Aryl-Substituted Quaternary Centers. *Angew. Chem., Int. Ed.* **2008**, *47*, 8211–8214. (h) Hawner, C.; Alexakis, A. Metal-catalyzed asymmetric conjugate addition reaction: formation of quaternary stereocenters. *Chem. Commun.* **2010**, *46*, 7295–7306. (i) Woodward, A. A. N. K. S. Copper-Catalyzed Asymmetric Conjugate Addition. In *Copper-Catalyzed Asymmetric Synthesis*; Alexakis, A., Krause, N., Woodward, S., Eds.; 2014; pp 33–68. (2) Takatsu, K.; Shintani, R.; Hayashi, T. Copper-Catalyzed 1,4-Addition of Organoboronates to Alkylidene Cyanoacetates: Mecha-

nistic Insight and Application to Asymmetric Catalysis. *Angew. Chem., Int. Ed.* **2011**, *50*, 5548–5552.

(3) Wu, C.; Yue, G.; Nielsen, C. D.-T.; Xu, K.; Hirao, H.; Zhou, J. Asymmetric Conjugate Addition of Organoboron Reagents to Common Enones Using Copper Catalysts. *J. Am. Chem. Soc.* **2016**, *138*, 742–745.

(4) (a) Hayashi, T.; Senda, T.; Ogasawara, M. Rhodium-Catalyzed Asymmetric Conjugate Addition of Organoboronic Acids to Nitroalkenes. *J. Am. Chem. Soc.* **2000**, *122*, 10716–10717. (b) Hayashi, T.; Takahashi, M.; Takaya, Y.; Ogasawara, M. Catalytic Cycle of Rhodium-Catalyzed Asymmetric 1,4-Addition of Organoboronic Acids. Aryl-rhodium, Oxa- π -allyl-rhodium, and Hydroxorhodium Intermediates. *J. Am. Chem. Soc.* **2002**, *124*, 5052–5058. (c) Hayashi, T.; Ueyama, K.; Tokunaga, N.; Yoshida, K. A Chiral Chelating Diene as a New Type of Chiral Ligand for Transition Metal Catalysts: Its Preparation and Use for the Rhodium-Catalyzed Asymmetric 1,4-Addition. *J. Am. Chem. Soc.* **2003**, *125*, 11508–11509. (d) Defieber, C.; Paquin, J.-F.; Serna, S.; Carreira, E. M. Chiral [2.2.2] Dienes as Ligands for Rh(I) in Conjugate Additions of Boronic Acids to a Wide Range of Acceptors. *Org. Lett.* **2004**, *6*, 3873–3876. (e) Paquin, J.-F.; Defieber, C.; Stephenson, C. R. J.; Carreira, E. M. Asymmetric Synthesis of 3,3-Diarylpropanals with Chiral Diene Rhodium Catalysts. *J. Am. Chem. Soc.* **2005**, *127*, 10850–10851. (f) Kina, A.; Yasuhara, Y.; Nishimura, T.; Iwamura, H.; Hayashi, T. Kinetic Studies Prove High Catalytic Activity of a Diene–Rhodium Complex in 1,4-Addition of Phenylboronic Acid to α,β -Unsaturated Ketones. *Chem. – Asian J.* **2006**, *1*, 707. (g) Duan, W.-L.; Iwamura, H.; Shintani, R.; Hayashi, T. Chiral Phosphine-Olefin Ligands in the Rhodium-Catalyzed Asymmetric 1,4-Addition Reactions. *J. Am. Chem. Soc.* **2007**, *129*, 2130–2138. (h) Shintani, R.; Takeda, M.; Nishimura, T.; Hayashi, T. Chiral Tetrafluorobenzobarrelenes as Effective Ligands for Rhodium-Catalyzed Asymmetric 1,4-Addition of Arylboroxines to β,β -Disubstituted α,β -Unsaturated Ketones. *Angew. Chem., Int. Ed.* **2010**, *49*, 3969–3971. (i) Wang, Z.-Q.; Feng, C.-G.; Zhang, S.-S.; Xu, M.-H.; Lin, G.-Q. Rhodium-Catalyzed Asymmetric Conjugate Addition of Organoboronic Acids to Nitroalkenes Using Chiral Bicyclo[3.3.0] Diene Ligands. *Angew. Chem., Int. Ed.* **2010**, *49*, 5780–5783. (j) Chen, G.; Gui, J.; Li, L.; Liao, J. Chiral Sulfoxide-Olefin Ligands: Completely Switchable Stereoselectivity in Rhodium-Catalyzed Asymmetric Conjugate Additions. *Angew. Chem., Int. Ed.* **2011**, *50*, 7681–7685. (k) He, Q.; Xie, F.; Fu, G.; Quan, M.; Shen, C.; Yang, G.; Gridnev, I. D.; Zhang, W. Palladium-Catalyzed Asymmetric Addition of Arylboronic Acids to Nitrostyrenes. *Org. Lett.* **2015**, *17*, 2250–2253. (l) Moku, B.; Fang, W.-Y.; Leng, J.; Kantchev, E. A. B.; Qin, H.-L. Rh(I)–Diene-Catalyzed Addition of (Hetero)aryl Functionality to 1,3-Dienylsulfonyl Fluorides Achieving Exclusive Regioselectivity and High Enantioselectivity: Generality and Mechanism. *ACS Catal.* **2019**, *9*, 10477–10488.

(5) (a) Gini, F.; Hessen, B.; Minnaard, A. J. Palladium-Catalyzed Enantioselective Conjugate Addition of Arylboronic Acids. *Org. Lett.* **2005**, *7*, 5309–5312. (b) Yamamoto, Y.; Nishikata, T.; Miyaura, N. 1,4-Additions of arylboron, -silicon, and -bismuth compounds to α,β -unsaturated carbonyl compounds catalyzed by dicationic palladium-(II) complexes. *Pure Appl. Chem.* **2008**, *80*, 807. (c) Miyaura, N. Celebrating 20 Years of SYNLETT - Special Account On Palladium-(II)-Catalyzed Additions of Arylboronic Acids to Electron-Deficient Alkenes, Aldehydes, Imines, and Nitriles. *Synlett* **2009**, 2039–2050. (d) Kikushima, K.; Holder, J. C.; Gatti, M.; Stoltz, B. M. Palladium-Catalyzed Asymmetric Conjugate Addition of Arylboronic Acids to Five-, Six-, and Seven-Membered Substituted Cyclic Enones: Enantioselective Construction of All-Carbon Quaternary Stereocenters. *J. Am. Chem. Soc.* **2011**, *133*, 6902–6905. (e) Holder, J. C.; Zou, L.; Marziale, A. N.; Liu, P.; Lan, Y.; Gatti, M.; Kikushima, K.; Houk, K. N.; Stoltz, B. M. Mechanism and Enantioselectivity in Palladium-Catalyzed Conjugate Addition of Arylboronic Acids to Substituted Cyclic Enones: Insights from Computation and Experiment. *J. Am. Chem. Soc.* **2013**, *135*, 14996–15007. (f) Liu, Y.; Han, S.-J.; Liu, W.-B.; Stoltz, B. M. Catalytic Enantioselective Construction of Quaternary Stereocenters: Assembly of Key Building Blocks for the

Synthesis of Biologically Active Molecules. *Acc. Chem. Res.* **2015**, *48*, 740–751. (g) Baek, D.; Ryu, H.; Ryu, J. Y.; Lee, J.; Stoltz, B. M.; Hong, S. Catalytic enantioselective synthesis of tetrasubstituted chromanones via palladium-catalyzed asymmetric conjugate arylation using chiral pyridine-dihydroisoquinoline ligands. *Chem. Sci.* **2020**, *11*, 4602–4607. (h) Wang, Z. Construction of all-carbon quaternary stereocenters by catalytic asymmetric conjugate addition to cyclic enones in natural product synthesis. *Org. Chem. Front.* **2020**, *7*, 3815–3841. (i) Bartáček, J.; Svoboda, J.; Kocúrik, M.; Pochobradský, J.; Čegan, A.; Sedláček, M.; Váňa, J. Recent advances in palladium-catalyzed asymmetric 1,4-additions of arylboronic acids to conjugated enones and chromones. *Beilstein J. Org. Chem.* **2021**, *17*, 1048–1085. (j) Baek, D.; Ryu, H.; Hahm, H.; Lee, J.; Hong, S. Palladium Catalysis Featuring Attractive Noncovalent Interactions Enabled Highly Enantioselective Access to β -Quaternary δ -Lactams. *ACS Catal.* **2022**, *12*, 5559–5564. (k) Lai, J.; Yang, C.; Csuk, R.; Song, B.; Li, S. Palladium Catalyzed Enantioselective Hayashi–Miyaura Reaction for Pharmaceutically Important 4-Aryl-3,4-dihydrocoumarins. *Org. Lett.* **2022**, *24*, 1329–1334.

(6) (a) Fagnou, K.; Lautens, M. Rhodium-Catalyzed Carbon–Carbon Bond Forming Reactions of Organometallic Compounds. *Chem. Rev.* **2003**, *103*, 169–196. (b) Hayashi, T.; Yamasaki, K. Rhodium-Catalyzed Asymmetric 1,4-Addition and Its Related Asymmetric Reactions. *Chem. Rev.* **2003**, *103*, 2829–2844. (c) Edwards, H. J.; Hargrave, J. D.; Penrose, S. D.; Frost, C. G. Synthetic applications of rhodium catalyzed conjugate addition. *Chem. Soc. Rev.* **2010**, *39*, 2093–2105. (d) Tian, P.; Dong, H.-Q.; Lin, G.-Q. Rhodium-Catalyzed Asymmetric Arylation. *ACS Catal.* **2012**, *2*, 95–119. (e) Li, Y.; Xu, M.-H. Simple sulfur–olefins as new promising chiral ligands for asymmetric catalysis. *Chem. Commun.* **2014**, *50*, 3771–3782. (f) Jia, T.; Cao, P.; Liao, J. Enantioselective synthesis of gem-diaryllkanes by transition metal-catalyzed asymmetric arylations (TMCAAr). *Chem. Sci.* **2018**, *9*, 546–559.

(7) (a) Shrestha, R.; Dorn, S. C. M.; Weix, D. J. Nickel-Catalyzed Reductive Conjugate Addition to Enones via Allylnickel Intermediates. *J. Am. Chem. Soc.* **2013**, *135*, 751–762. (b) Weix, D. J. Methods and Mechanisms for Cross-Electrophile Coupling of Csp² Halides with Alkyl Electrophiles. *Acc. Chem. Res.* **2015**, *48*, 1767–1775.

(8) (a) Chen, J.; Wang, Y.; Ding, Z.; Kong, W. Synthesis of bridged tricyclo[5.2.1.0.1,5]decenes via nickel-catalyzed asymmetric domino cyclization of enynones. *Nat. Commun.* **2020**, *11*, 1882. (b) Zhang, S.; Pervene, S.; Ouyang, Y.; Xu, L.; Yu, T.; Zhao, M.; Wang, L.; Song, P.; Li, P. Design and Synthesis of Tunable Chiral 2,2'-Bipyridine Ligands: Application to the Enantioselective Nickel-Catalyzed Reductive Arylation of Aldehydes. *Angew. Chem., Int. Ed.* **2022**, *61*, No. e202117843. (c) Zhu, Z.; Xiao, J.; Li, M.; Shi, Z. Nickel-Catalyzed Intermolecular Asymmetric Addition of Aryl Iodides across Aldehydes. *Angew. Chem., Int. Ed.* **2022**, *61*, No. e202201370.

(9) Pellissier, H. Recent Developments in Enantioselective Nickel-(II)-Catalyzed Conjugate Additions. *Adv. Synth. Catal.* **2015**, *357*, 2745–2780.

(10) (a) Hickey, D. P.; Sandford, C.; Rhodes, Z.; Gensch, T.; Fries, L. R.; Sigman, M. S.; Minter, S. D. Investigating the Role of Ligand Electronics on Stabilizing Electrocatalytically Relevant Low-Valent Co(I) Intermediates. *J. Am. Chem. Soc.* **2019**, *141*, 1382–1392. (b) Li, W.; Wang, G.; Lai, J.; Li, S. Multifunctional isouquinoline-oxazoline ligands of chemical and biological importance. *Chem. Commun.* **2019**, *55*, 5902–5905. (c) Ping, Y.; Wang, K.; Pan, Q.; Ding, Z.; Zhou, Z.; Guo, Y.; Kong, W. Ni-Catalyzed Regio- and Enantioselective Domino Reductive Cyclization: One-Pot Synthesis of 2,3-Fused Cyclopentannulated Indolines. *ACS Catal.* **2019**, *9*, 7335–7342.

(11) Cabrera, A.; Le Lagadec, R.; Sharma, P.; Luis Arias, J.; Alfredo Toscano, R.; Velasco, L.; Gaviño, R.; Alvarez, C.; Salmón, M. Cyclo- and hydrodimerization of α,β -unsaturated ketones promoted by samarium diiodide. *J. Chem. Soc., Perkin Trans. 1* **1998**, 3609–3618.

(12) (a) Hucklenbroich, J.; Klein, R.; Neumaier, B.; Graf, R.; Fink, G. R.; Schroeter, M.; Rueger, M. A. Aromatic-turmerone induces neural stem cell proliferation in vitro and in vivo. *Stem Cell Res. Ther.* **2014**, *5*, a100. (b) Saga, Y.; Hatakenaka, Y.; Matsumoto, M.;

Yoshioka, Y.; Matsumura, S.; Zaima, N.; Konishi, Y. Neuroprotective effects of aromatic turmerone on activity deprivation-induced apoptosis in cerebellar granule neurons. *NeuroReport* **2020**, *31*, 1302–1307. (c) Hori, Y.; Tsutsumi, R.; Nasu, K.; Boateng, A.; Ashikari, Y.; Sugiura, M.; Nakajima, M.; Kurauchi, Y.; Hisatsune, A.; Katsuki, H.; Seki, T. Aromatic-Turmerone Analogs Protect Dopaminergic Neurons in Midbrain Slice Cultures through Their Neuroprotective Activities. *Cell* **2021**, *10*, a1090.

(13) (a) Chen, G.; Tokunaga, N.; Hayashi, T. Rhodium-Catalyzed Asymmetric 1,4-Addition of Arylboronic Acids to Coumarins: Asymmetric Synthesis of (R)-Tolterodine. *Org. Lett.* **2005**, *7*, 2285–2288. (b) Gallagher, B. D.; Taft, B. R.; Lipshutz, B. H. Asymmetric Conjugate Reductions of Coumarins. A New Route to Tolterodine and Related Coumarin Derivatives. *Org. Lett.* **2009**, *11*, 5374–5377.

(14) Cumming, J. G.; Tucker, H.; Oldfield, J.; Fielding, C.; Highton, A.; Faull, A.; Wild, M.; Brown, D.; Wells, S.; Shaw, J. Balancing hERG affinity and absorption in the discovery of AZD5672, an orally active CCR5 antagonist for the treatment of rheumatoid arthritis. *Bioorg. Med. Chem. Lett.* **2012**, *22*, 1655–1659.

(15) Jia, X.-G.; Guo, P.; Duan, J.; Shu, X.-Z. Dual nickel and Lewis acid catalysis for cross-electrophile coupling: the allylation of aryl halides with allylic alcohols. *Chem. Sci.* **2018**, *9*, 640–645.

(16) (a) Yin, H.; Fu, G. C. Mechanistic Investigation of Enantioconvergent Kumada Reactions of Racemic α -Bromoketones Catalyzed by a Nickel/Bis(oxazoline) Complex. *J. Am. Chem. Soc.* **2019**, *141*, 15433–15440. (b) Ju, L.; Lin, Q.; LiBretto, N. J.; Wagner, C. L.; Hu, C. T.; Miller, J. T.; Diao, T. Reactivity of (bi-Oxazoline)organonickel Complexes and Revision of a Catalytic Mechanism. *J. Am. Chem. Soc.* **2021**, *143*, 14458–14463. (c) Wagner, C. L.; Herrera, G.; Lin, Q.; Hu, C. T.; Diao, T. Redox Activity of Pyridine-Oxazoline Ligands in the Stabilization of Low-Valent Organonickel Radical Complexes. *J. Am. Chem. Soc.* **2021**, *143*, 5295–5300.

(17) Dorigo, A. E.; Morokuma, K. Theoretical studies of nucleophilic additions of organocopper reagents to acrolein. Rationalization of the differences in regioselectivity in the reactions of methylcopper and methyllithium. *J. Am. Chem. Soc.* **1989**, *111*, 4635–4643.

(18) Cordero, B.; Gómez, V.; Platero-Prats, A. E.; Revés, M.; Echeverría, J.; Cremades, E.; Barragán, F.; Alvarez, S. Covalent radii revisited. *Dalton Trans.* **2008**, 2832–2838.

(19) (a) Nishikata, T.; Yamamoto, Y.; Gridnev, I. D.; Miyaura, N. Enantioselective 1,4-Addition of Ar_3Bi , $[\text{ArBF}_3]\text{K}$, and ArSiF_3 to Enones Catalyzed by a Dicationic Palladium(II)–Chiraphos or –Dipamp Complex. *Organometallics* **2005**, *24*, 5025–5032. (b) Mauleón, P.; Alonso, I.; Rivero, M. R.; Carretero, J. C. Enantioselective Synthesis of Chiral Sulfones by Rh-Catalyzed Asymmetric Addition of Boronic Acids to α,β -Unsaturated 2-Pyridyl Sulfones. *J. Org. Chem.* **2007**, *72*, 9924–9935. (c) Lan, Y.; Houk, K. N. Mechanism of the Palladium-Catalyzed Addition of Arylboronic Acids to Enones: A Computational Study. *J. Org. Chem.* **2011**, *76*, 4905–4909. (d) Peng, Q.; Yan, H.; Zhang, X.; Wu, Y.-D. Conjugate Addition vs Heck Reaction: A Theoretical Study on Competitive Coupling Catalyzed by Isoelectronic Metal (Pd(II) and Rh(I)). *J. Org. Chem.* **2012**, *77*, 7487–7496. (e) Boeser, C. L.; Holder, J. C.; Taylor, B. L. H.; Houk, K. N.; Stoltz, B. M.; Zare, R. N. Mechanistic analysis of an asymmetric palladium-catalyzed conjugate addition of arylboronic acids to β -substituted cyclic enones. *Chem. Sci.* **2015**, *6*, 1917–1922.

(20) Harutyunyan, S. R.; López, F.; Browne, W. R.; Correa, A.; Peña, D.; Badorrey, R.; Meetsma, A.; Minnaard, A. J.; Feringa, B. L. On the Mechanism of the Copper-Catalyzed Enantioselective 1,4-Addition of Grignard Reagents to α,β -Unsaturated Carbonyl Compounds. *J. Am. Chem. Soc.* **2006**, *128*, 9103–9118.

Recommended by ACS

Palladium-Catalyzed Enantioselective $\text{C}(\text{sp}^3)\text{--H}$ Arylation of 2-Propyl Azaaryls Enabled by an Amino Acid Ligand

Hong-Liang Li, Yoichiro Kuninobu, *et al.*

FEBRUARY 10, 2022
ORGANIC LETTERS

READ 

Efficient Enantio-, Diastereo-, *E/Z*-, and Site-Selective Nickel-Catalyzed Fragment Couplings of Aldehydes, Dienes, and Organoborons

Justin S. Marcum and Simon J. Meek

OCTOBER 04, 2022
JOURNAL OF THE AMERICAN CHEMICAL SOCIETY

READ 

Nickel-Catalyzed Enantioselective Coupling of Aldehydes and Electron-Deficient 1,3-Dienes Following an Inverse Regiochemical Course

Thomas Q. Davies, Alois Fürstner, *et al.*

OCTOBER 04, 2022
JOURNAL OF THE AMERICAN CHEMICAL SOCIETY

READ 

Asymmetric Intermolecular Iodination Difunctionalization of Allylic Sulfonamides Enabled by Organosulfide Catalysis: Modular Entry to Iodinated Chiral Molecules

Lihao Liao, Xiaodan Zhao, *et al.*

SEPTEMBER 02, 2022
JOURNAL OF THE AMERICAN CHEMICAL SOCIETY

READ 

Get More Suggestions >